SPECTRAL CHARACTERISTICS OF MERCURY'S PYROCLASTIC DEPOSITS: ANALYSIS OF CHARACTERISTIC PARAMETERS AND SPATIAL VARIATION. C. L. Olson[1,2], N. R. Izenberg[1], and L. M. Jozwiak[1], [1]Johns Hopkins University Applied Physics Laboratory, Laurel, MD, USA, [2] University of Maryland, College Park, MD, USA. (corresponding author: olson.caroline@comcast.net)

Introduction: From 2008-2015, flyby, and then orbital images from the MESSENGER spacecraft revealed the presence of pyroclastic deposits on Mercury's surface [1]. Following the end of orbital operations, a final total of 103 deposits were documented and catalogued in [2]. Of these 103 deposits, 85 had been observed by the Visible and Infrared Spectrograph (VIRS) component of the Mercury Atmospheric and Surface Composition Spectrometer (MASCS) instrument onboard the MESSENGER spacecraft [3]. In 2014, Goudge et al. [4] used the available VIRS data, usually just a single observation for each deposit, to characterize the spectral signatures of the 40 recognized pyroclastic deposits. Goudge et al. [4] identified two main diagnostic parameters for pyroclastic deposits: the UV absorption depth and the reflectance at 700 nm.

In this work, we seek to update this analysis utilizing the full VIRS dataset acquired during the MESSENGER mission, and examining the full catalog of recognized pyroclastic deposits [2]. We investigate the spectral characteristics of pyroclastic deposits, and global spatial variations in these parameters.

Methods: Goudge et al. [4] suggested that the main spectral characteristics of pyroclastic deposits (UV absorption depth and reflectance at 700 nm) were related to either variations in deposit composition or the space weathering of the deposit. Using this hypothesis as a guide, we looked at parameters likely to be indicative of composition or degree of weathering. Nine such parameters were chosen, and their derivation and rationale are listed below.

Reflectance at 575 nm (R575): proxy for age/degree of space weathering, used previously for studies of the moon and Mercury [5].

Reflectance at 700 nm (R700): proxy for age/degree of space weathering, reflectance value used in [4] to define spectral types of pyroclastic vents

UV Ratio (UVr): ratio of reflectance at 310 nm to reflectance at 390 nm, measure of the steepness of the UV absorption (a region associated with the oxygen-metal charge transfer), proxy for metal content [4, 5].

IR Ratio (IRr): ratio of reflectance at 415 nm to reflectance at 720 nm, captures the curvature in the visible and infrared, unaffected by UV absorption.

Red/Blue Ratio (RBr): similar to IR ratio, ratio of reflectance at 770 nm to reflectance at 440 nm [5, 6], associated with presence of nanoparticulate iron oxides.

Band Depth at 530 nm (BD530): measure of the depth of an absorption band at 530 nm, higher values indicate more fine-grained crystal hematite [5, 6], calculated with the equation:

$$\mathrm{BD530} = 1 - \left(\frac{R530}{0.517 * R614 + 0.483 * R440}\right)$$

Shoulder Height at 400 nm (SH400): measure of one side of the absorption band at 400 nm, a less accurate assessment on the UV absorption band associated with the oxygen-metal charge transfer calculated with:

$$\mathrm{SH400} = 1 - \left(\frac{0.500 * R350 + 0.500 * R450}{R400}\right)$$

Shoulder Height at 600 nm (SH600): measure of one side of an absorption band at 600 nm, associated with select ferric minerals or sulfur, from [5, 6] calculated with:

$$\mathrm{SH600} = 1 - \left(\frac{0.366 * R533 + 0.634 * R716}{R600}\right)$$

UV Depth: measure of the strength of the UV downturn, similar to UV Ratio, associated with oxygen-metal charge transfer, used to define types of pyroclastic vents in [4], calculated using equations 1-5 in [4].

Analysis: We compared the global set of pyroclastic vents [2] several different ways in order to search for differences in parameters. Categorization methods are listed below.

"Goudge type": Goudge et al. [4] identified 4 spectral categories of pyroclastic vents based on their UV Depth parameter (similar to our UV Ratio, although ours is simpler to derive). Divisions were based on the mean and standard deviation of the set of UV depth parameters. Type 1 included vents with the lowest UV depths, and type 4 included vents with the highest UV depths. [4]

North/South: These categories consist of all of the vents in latitudes above 0° (north) and vents in latitudes below 0° (south).

East/West: Similar to North/South categories, east consists of vents in the eastern hemisphere and west vents in the western hemisphere, divided along 0° longitude.

Target Regions: Initial trends observed in the above location divisions suggested more specific regions may reveal more specific trends. The Caloris Basin, the High Magnesium Region (HMR) [7], a southeast region of low reflectance material (SE LRM) [8], the Hesiod region, and a northeastern region of pyroclastic material were all studied as separate regions. Details of each region are shown in Table 1.

Using the MESSENGER mission Quickmap tool [9], we selected 5-20 VIRS spectra located on each pyroclastic deposit and derived average parameter values. Also using quickmap, we derived 'background surface' parameters using 5 VIRS spectra located on near the deposit

but free of pyroclastic material, and representative of the surrounding terrain. We used the background spectra to create a deposit vs. background material ratio value for each parameter. Mercury has different geologic and spectral provinces [5, 10], and these ratios allowed us to focus on differences in the deposit itself rather than differences in the composition of its region.

Region	Latitude Range	Longitude Range	# of Pyro Deposits
Caloris Basin	10° to 55°	140° to 190°	9
HMR	-30° to 60°	210° to 330°	19
SE LRM	-60° to 0°	0° to 105°	11
Hesiod	-66° to -21°	270° to 360°	7
NE Pyro	25° to 75°	35° to 115°	5

Table 1: *Location and number of pyroclastic deposits located in each of the five target regions.*

Results: As seen by Goudge et al. [4], we found that much of the variation between the pyroclastic spectral types is in the UV and the visible and near-infrared reflectance. In initial studies, trends in the UV ratio and reflectance at 700 nm are similar to the trends observed in [4] (Figure 1). However, when using the deposit to background material ratios, Type 1 deviates from the trend (Figure 2), indicating a compositional variation from the other deposit types.

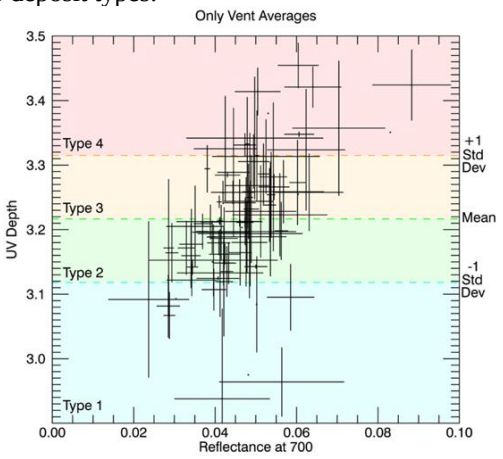

Figure 1: *The divisions of each Goudge type in R700 and UV Depth parameters. Type 1 tends to have the lowest values of those parameters, and Type 4 the highest.*

Though the initial categorization was somewhat arbitrary, we found that deposits in the southern hemisphere tended to have lower reflectance values and higher UV and IR ratios. We found similar trends in east-west categorization; deposits in the eastern hemisphere tended to have lower reflectance values and higher UV and IR ratios. These trends are likely due to compositional differences across large regions located largely in one hemisphere or the other, and would be better investigated through the isolation of deposits located in those known regions.

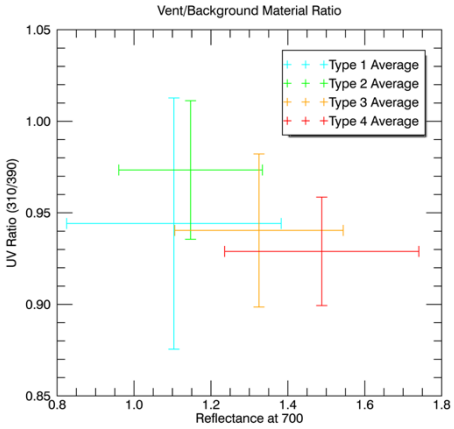

Figure 2: *The Goudge types in reflectance at 700 and UV Ratio parameters. Type 1 deviates from the expected trend.*

Of the five target regions, the Hesiod region, HMR, and NE pyroclastic region showed no distinct grouping in any of the parameters. However, deposits in the SE LRM region have similar reflectance values, UV ratios, and IR ratios. This grouping in the UV and IR ratios is shown in figure 3 (left), and suggests that deposits in this region may be of similar age and composition (specifically metallicity), distinct from other mercurian deposits. Trends were also observed in deposits located in the Caloris Basin, in both reflectance and the shoulder height at 600 nm, shown in figure 3 (right). Grouping in reflectance suggests that the deposits are of similar age, and the deposit's comparatively low values in the shoulder height at 600 indicate a different compositional source region for those deposits.

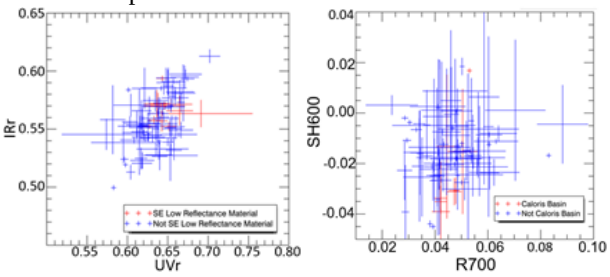

Figure 3: *Left) UV Ratio plotted against IR Ratio of all pyroclastic deposits, with those in the SE LRM region in red. SE LRM deposits group in the mid-range of each parameter. Right) R700 nm plotted against the SH600 parameter, with deposits in the Caloris Basin in red grouping distinctly with mid-range reflectance values and low shoulder height.*

References: [1] Head, J. W., et al. (2008) *Science 321*, 69-72. [2] Jozwiak et al. (2018) *Icarus 302*, 191-212. [3] McClintock and Lankton (2007), SSR, 131, 481-522. [4] Goudge et al. (2014) *JGR, 119(3)*, 635–658. [5] Izenberg et al. (2014) *Icarus, 228*, 364–374. [6] VivianoBeck et al. (2014) *JGR*, 119(6), 1403–1431. [7] Weider, S. Z., et al. (2015) *EPSL 416*, 109-120. [8] Murchie, S. L., et al. (2015) *Icarus 254*, 287-305. [9] MESSENGER Quickmap orbital data tool: messenger.jhuapl.edu/Explore/Quick-Map-Orbital-Data.html. [10] Denevi et al. (2009) *Science* 324:613.